

Ni self-diffusion in refractory Al-Ni meltsS. Stüber,¹ D. Holland-Moritz,² T. Unruh,³ and A. Meyer²¹*Physik Department E13, Technische Universität München, 85747 Garching, Germany*²*Institut für Materialphysik im Weltraum, Deutsches Zentrum für Luft- und Raumfahrt (DLR), 51170 Köln, Germany*³*Forschungsneutronenquelle Heinz Maier-Leibnitz (FRM II), Technische Universität München, 85747 Garching, Germany*

(Received 10 August 2009; revised manuscript received 11 December 2009; published 26 January 2010)

This work presents investigations on the Ni self-diffusion coefficient in Al-Ni melts forming the technological relevant intermetallic phases Al₅₀Ni₅₀ and Al₂₅Ni₇₅ by quasielastic neutron scattering. We found that the Ni self-diffusivity at constant temperature is nearly independent of the composition within the composition range between 0 and 50 at. % Al. This may be a result of the small composition dependence of the atomic volume observed in the same range of composition.

DOI: [10.1103/PhysRevB.81.024204](https://doi.org/10.1103/PhysRevB.81.024204)

PACS number(s): 61.25.Mv, 66.30.Fq, 61.05.fg

I. INTRODUCTION

The properties of materials produced by solidification from melts are governed by microscopic scale processes such as crystal nucleation and subsequent crystal growth. Of these processes, especially crystal growth is strongly dependent on the atomic diffusion in the liquid phase.^{1–4} For alloy melts, in most cases the composition of the crystallizing solid phase differs from that of the liquid phase (partitioning) and hence it is immediately obvious that mass transport plays an important role during solidification limiting the crystal growth velocity. Indeed, measurements of the growth velocities as function of the undercooling of the melt have revealed significantly lower growth velocities for partitioning alloys as compared to pure metals at similar levels of undercooling.^{5,6} Also for congruently melting intermetallic AlNi and AlTi alloys investigations of the solidification behavior of deeply undercooled liquids revealed dendrite growth velocities that are one to two orders of magnitude smaller than growth velocities observed in melts of pure metals at similar undercoolings.^{7,8} During solidification of intermetallic phases, the atomic attachment of atoms from the liquid to the solid requires short-range atomic diffusion, because the atoms have to sort them out to find the proper lattice site in the superlattice structure. Consequently, atomic diffusion decisively influences the crystal growth of intermetallic phases, even for congruently melting systems. This is supported by recent molecular dynamics (MD) simulations that provide evidence that growth of the intermetallic B2 phase is controlled by diffusive mass transport at the solid-liquid interface.⁹

Hence, in order to describe the crystal growth in alloy melts and to test existing growth models¹⁰ the knowledge of self-diffusion coefficients in the melt is a prerequisite. It should be stressed that for nonequilibrium solidification processes from undercooled melts, solidification occurs at temperatures below the melting temperature and consequently, in order to model of such processes the diffusion coefficients must be known at temperatures within the metastable regime of undercooled melts.

A possibility to measure diffusion coefficients in liquids is offered by capillary methods where the development of concentration profiles within the capillary as function of time is

analyzed.¹¹ If not performed under microgravity conditions, such measurements may be hampered by buoyancy-driven convective flow. Moreover, chemical reactions of the melt with the capillary material limit the applicability of the method. These problems can be circumvented by the use of quasielastic neutron scattering (QNS).¹² Here, the self-diffusion of a single component can be accessed from *equilibrium* fluctuations, if the incoherent scattering from that component dominates the low-wave-number response. QNS probes the dynamics on atomic length scales and on a picosecond time scale; short enough to be undisturbed by the presence of convection flow. Comparative measurements of the Ni self-diffusivity in Pd₄₀Cu₃₀Ni₁₀P₂₀ alloy melts by QNS (Ref. 12) and by use of a shear cell technique under microgravity¹³ have demonstrated that both different methods deliver results that are identical within the error limits at the same temperature.¹³

In this paper we present a QNS study of the atomic dynamics in binary Al-Ni alloys. The Al-Ni alloy system is of high technological interest because it is a basis system for superalloys characterized by a high thermal stability (e.g., Al₂₅Ni₇₅) and containing also the refractory intermetallic Al₅₀Ni₅₀ with a rather high liquidus temperature of 1940 K. Al-Ni alloys are known to exhibit a chemical short-range order in the liquid phase.^{14,15} In diffraction measurements, this can be seen as a prepeak in the coherent contribution to the static structure factor. The structure and the atomic dynamics in the Al-Ni system have been the object of considerable experimental^{14,16,17} and theoretical^{9,18–20} work. It was found by QNS experiments and MD simulations¹⁵ that the Ni self-diffusion coefficients exhibit a nonlinear dependence on concentration with a pronounced increase on the Al-rich side.

In the preceding experimental studies¹⁷ on the atomic dynamics in Al-Ni alloys the samples have been molten within a crucible. The thermal stability of the crucibles as well as chemical reactions of the crucible materials with the melt restrict the accessible temperatures on the high-temperature side, prohibiting, for instance, the investigation of refractory Al₅₀Ni₅₀ melts because of their high melting temperature. The lower limit of the temperature range is given by heterogeneous nucleation at the crucible walls that prevents to undercool the liquids significantly below the melting temperature. Moreover, scattering at the crucible material deteriorates the achievable signal to background ratio.

In order to overcome these crucible-related problems, in this work the samples have been processed containerlessly by application of the electromagnetic levitation technique.²¹ We have chosen the alloy compositions $\text{Al}_{50}\text{Ni}_{50}$ and $\text{Al}_{25}\text{Ni}_{75}$ for our studies that correspond to the compositions of the technologically interesting intermetallic solid phases.

II. EXPERIMENTAL DETAILS

$\text{Al}_{50}\text{Ni}_{50}$ and $\text{Al}_{25}\text{Ni}_{75}$ samples, approximately 8 mm in diameter, were prepared from the constituents under an Ar atmosphere (purity 99.9999%) by arc melting. In order to deeply undercool the liquids below the melting temperature and in order to avoid reactions of the chemically highly reactive Al-based melts with crucible materials, the liquids are containerlessly processed within a He atmosphere of 99.9999% purity by utilizing the electromagnetic levitation technique. The roughly spherical, electrically conductive sample is inductively heated and levitated within an inhomogeneous electromagnetic rf field that is generated by a levitation coil system. A specially designed electromagnetic levitator was used, that was already employed in preceding neutron-diffraction studies on the short-range order of undercooled metallic melts²² and that has recently been modified in order to perform also quasielastic neutron-scattering experiments.²³ In this setup a levitation coil system with a wide gap between the lower and upper windings is employed that allows to illuminate the whole sample with neutrons such that the scattering geometry is resistant to small fluctuations of the sample position.

The sample temperature is measured by a one color pyrometer using a constant emissivity that is adjusted such that the melting temperatures of the samples agree with the known values of the sample material. The accuracy of the measured temperatures is estimated to ± 5 K.

The quasielastic neutron-scattering experiments were performed at the time of flight spectrometer TOFTOF (Ref. 24) at the Forschungsneutronenquelle Heinz Maier-Leibnitz (FRM II). An incoming wavelength of the neutrons of 5.4 Å was used. The instrumental energy resolution function $R(q, \omega)$, measured at 300 K using a vanadium standard of similar size can be well approximated by a Gaussian function with a full width at half maximum (FWHM) at zero-energy transfer of 78 μeV .

Figure 1 shows a raw time-of-flight spectrum measured for an $\text{Al}_{50}\text{Ni}_{50}$ melt at $T=1840$ K that was acquired within a range of scattering angles of $39^\circ < 2\theta < 55^\circ$. Also shown is the spectrum of the empty levitator. Due to the containerless processing setup the background is one to two orders of magnitude smaller than the signal measured with sample. After subtraction of the background, the raw spectra are normalized to a vanadium standard and corrected for self-absorption. In order to obtain the scattering law $S(q, \omega)$ the corrected data were interpolated to constant q and symmetrized with respect to energy with the detailed balance factor.

The wavelength used gives access to a range of (elastic) momentum transfer of $0.4 < q < 2.2$ Å⁻¹, which is below the first structure factor maximum of the Ni-Al system.¹⁵ This reduces strongly the contribution of coherent scattering and

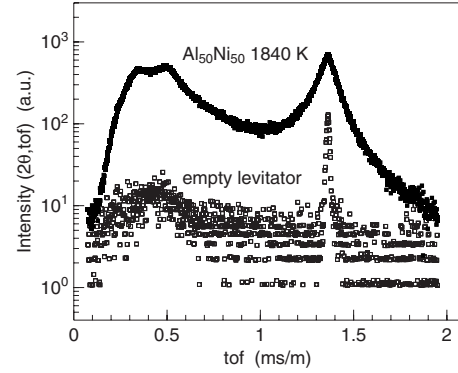


FIG. 1. Time-of-flight spectra measured for an $\text{Al}_{50}\text{Ni}_{50}$ melt at $T=1840$ K and for the empty levitator. The spectra cover a range of scattering angles of $39^\circ < 2\theta < 55^\circ$.

hence, influences of multiple scattering on the signal are negligible. Typical measurement times were 2–3 h per temperature and sample.

It has been verified that even for strongly incoherent scattering samples like those of pure Ni and Ti, the precise determination of diffusion coefficients is not hampered by influences of multiple scattering, despite of the sample geometry [diameter approximately 8 mm (Refs. 23 and 25)]. The data treatment procedure is described in detail in Refs. 23, 25, and 26.

III. RESULTS AND DISCUSSION

Figure 2 shows the measured scattering laws $S(q, \omega)$ for liquid (a) $\text{Al}_{25}\text{Ni}_{75}$ at $T=1868$ K and (b) $\text{Al}_{50}\text{Ni}_{50}$ at $T=1840$ K, both for $q=0.6$ and 1.2 Å⁻¹. Please note the logarithmic ordinate. In both cases the quasielastic line broadens with increasing q .

For small momentum transfer (below $q \approx 1.4$ Å⁻¹) the measured signal is dominated by the incoherent scattering of the Ni atoms [incoherent scattering cross-sections: $\sigma_{\text{inc}}(\text{natNi})=5.2$ b and $\sigma_{\text{inc}}(\text{Al})=0.0082$ b] and the scattering law for the diffusion of Ni in the melt, in the hydrodynamic regime of low-momentum transfer is described by a Lorentzian function^{27–30}

$$S_{\text{inc}}(q, \omega) = \frac{A}{\pi \hbar} \frac{Dq^2}{(Dq^2)^2 + \omega^2} + b_q.$$

Here, D denotes the self-diffusion coefficient of Ni that is the dominant incoherent scattering contributor, A a proportionality factor, containing, among others, number density of scatterers and typical path length of neutrons through the sample, and b_q a (q dependent) background which accounts for contributions of phononic vibrations and remaining coherent scattering that are assumed constant in the fitting range. The solid lines in Fig. 2 are fits to the measured data, using the scaled Lorentz function convoluted with the instrumental energy resolution (FWHM 78 μeV).

For a diffusing ideal incoherent scatterer, the half width at half maximum $\Gamma_{1/2}$ of the Lorentzian function is linked with the self-diffusivity of the scatterer: $D = \Gamma_{1/2} / (\hbar q^2)$. For

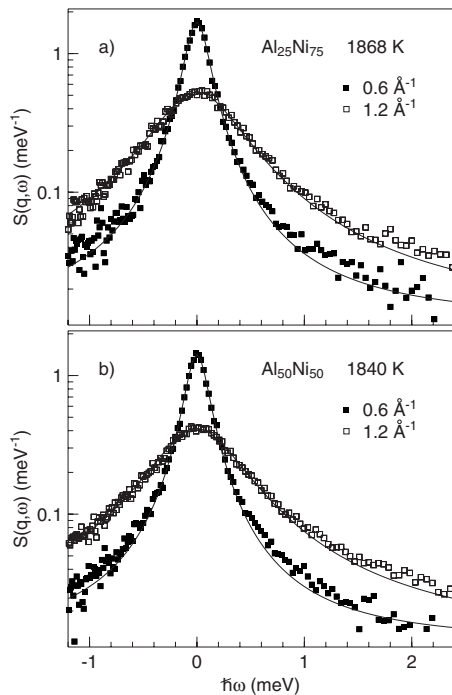


FIG. 2. Scattering law $S(q, \omega)$ of liquid (a) $\text{Al}_{25}\text{Ni}_{75}$ at $T=1868$ K and (b) $\text{Al}_{50}\text{Ni}_{50}$ at $T=1840$ K, both for $q=0.6$ and 1.2 \AA^{-1} . The lines are fits with a Lorentz function that is convoluted with the instrumental energy resolution.

$\text{Al}_{50}\text{Ni}_{50}$ the half width at half maximum $\Gamma_{1/2}$ of $S_{\text{inc}}(q, \omega)$ is plotted in Fig. 3 for different temperatures as a function of q^2 . $\Gamma_{1/2}$ shows a linear dependence on q^2 up to a value of $q^2 \approx 1.6 \text{ \AA}^{-2}$, above which the increasing contribution of coherent scattering cannot be neglected anymore. From the slopes of the linear fits (Fig. 3) the Ni self-diffusivities are determined. The results for the melts of $\text{Al}_{50}\text{Ni}_{50}$ and $\text{Al}_{25}\text{Ni}_{75}$ at different temperatures are given in Table I together with results from former experiments in a crucible on $\text{Al}_{25}\text{Ni}_{75}$.

For the determination of the Ni self-diffusion coefficients the data are analyzed in the framework of hydrodynamics, which predicts a Lorentzian shape of the scattering law as

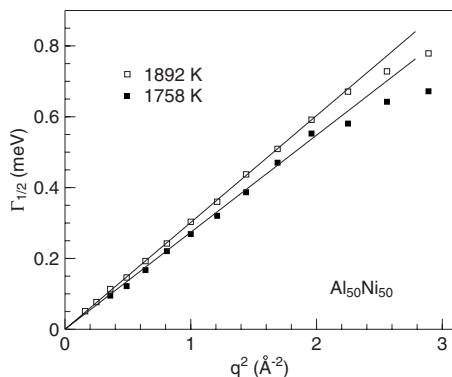


FIG. 3. q -dependent half width at half maximum $\Gamma_{1/2}$ of the scattering law $S(q, \omega)$ for $\text{Al}_{50}\text{Ni}_{50}$ at two different temperatures. The lines are linear fits for $q^2 < 1.6 \text{ \AA}^{-2}$, from which the Ni self-diffusion coefficients are determined.

well as a linear dependence of its half width on q^2 at small q . Indeed the experimentally determined scattering law is well described by a Lorentzian function (Fig. 2) and a linear dependence of $\Gamma_{1/2}$ is observed for $q^2 < 1.6 \text{ \AA}^{-2}$, indicating that the hydrodynamic approximation is justified in this range of momentum transfer. The question on the validity of the hydrodynamic approximation has also recently been addressed by QNS and molecular dynamics simulations for the example of liquid Ti.²⁵ It has been shown that for liquid Ti this approximation is justified for $q < 1.2 \text{ \AA}^{-1}$ ($q^2 < 1.44 \text{ \AA}^{-2}$). The molecular-dynamics simulations allow to determine the purely incoherent dynamic structure factor from which the self-diffusion coefficient can be calculated. Alternatively, the self-diffusion coefficient can be estimated from the long-time limit of the mean square displacement of the atomic positions. Both methods deliver consistent results. The molecular-dynamics simulations also show that the hydrodynamic description can be applied for $q < 1.2 \text{ \AA}^{-1}$, which is in agreement with the QNS results on liquid Ti.

In Fig. 4 the diffusion coefficients determined by QNS are plotted as function of the inverse temperature. In semilogarithmic representation the measured diffusion constants lie on a straight line, indicating that in the investigated temperature range the Ni self-diffusion is well described by an Arrhenius law: $D=D_0 \exp(-E_A/k_B T)$. Here E_A denotes the activation energy of the diffusion process and D_0 a temperature-independent prefactor. For $\text{Al}_{50}\text{Ni}_{50}$ we find $E_A=0.42$ eV per atom and $D_0=60 \times 10^{-9} \text{ m}^2 \text{ s}^{-1}$ and for $\text{Al}_{25}\text{Ni}_{75}$ $E_A=0.465$ eV per atom and $D_0=78 \times 10^{-9} \text{ m}^2 \text{ s}^{-1}$. The data points for $\text{Al}_{25}\text{Ni}_{75}$ comprise the results of this work and of former quasielastic neutron-scattering experiment in a crucible.¹⁷ All these data points are on the same line, again highlighting the reliability of the levitation approach.

Figure 4 also shows that at a given temperature the Ni self-diffusivities measured for pure Ni, $\text{Al}_{25}\text{Ni}_{75}$ and $\text{Al}_{50}\text{Ni}_{50}$ are similar indicating that the Ni self-diffusivities are essentially independent of the alloy composition, in the composition range between 0 and 50 at. % Al. It is also remarkable that—though the measurements on the Ni-rich alloys are all in the same absolute temperature range—the liquidus temperatures of these alloys are quite different, $T_L=1940$ K for $\text{Al}_{50}\text{Ni}_{50}$, $T_L=1658$ K for $\text{Al}_{25}\text{Ni}_{75}$, and $T_L=1726$ K for pure Ni. Hence, the Ni self-diffusivities of $\text{Al}_{50}\text{Ni}_{50}$ were determined in the metastable regime of an undercooled melt, whereas for $\text{Al}_{25}\text{Ni}_{75}$, the Ni self-diffusion coefficient was measured well above the liquidus temperature within the stable melt. The data for pure Ni was measured in both states. No change in slope in the temperature dependence of the Ni self-diffusivity is observed at the melting temperature.

In the upper part of Fig. 5 we compare the Ni self-diffusivities measured in this work and in the preceding studies¹⁷ at the same temperature of $T=1795$ K as a function of the alloy compositions including also data on the Al-rich side. As discussed before, the Ni self-diffusivity is nearly independent of the composition on the Ni-rich side up to 50 at. % Al. On the Al-rich side, however, the addition of Al leads to a drastic monotonic increase in the Ni self-diffusivity. In order to analyze if there is any relation to the phase diagram, we inspect the concentration dependence of the Ni self-diffusion of the studied Al-Ni alloys at their re-

TABLE I. Ni self-diffusion coefficients determined by quasielastic neutron scattering for $\text{Al}_{25}\text{Ni}_{75}$ and $\text{Al}_{50}\text{Ni}_{50}$.

Alloy	T_L (K)	T (K)	D (this work) ($\times 10^{-9} \text{ m}^2 \text{ s}^{-1}$)	D [crucible (Ref. 17)] ($\times 10^{-9} \text{ m}^2 \text{ s}^{-1}$)	E_A (eV per atom)	D_0 ($\times 10^{-9} \text{ m}^2 \text{ s}^{-1}$)
$\text{Al}_{25}\text{Ni}_{75}$	1658	1670 ± 5		3.05 ± 0.17	0.465 ± 0.027	78 ± 13
		1689 ± 5	3.22 ± 0.08			
		1795 ± 5		3.95 ± 0.10		
		1868 ± 5	4.35 ± 0.05			
		1928 ± 5	4.90 ± 0.20			
$\text{Al}_{50}\text{Ni}_{50}$	1940	1758 ± 5	3.7 ± 0.3		0.42 ± 0.06	60 ± 22
		1840 ± 5	4.35 ± 0.17			
		1892 ± 5	4.59 ± 0.11			

spective liquidus temperature as a function of the Ni content that is shown in the bottom part of Fig. 5.

For intermediate concentrations, the higher liquidus temperature of the intermetallic causes a moderate increase in the diffusivity. The activation energies are fairly equal, with somewhat lower values on the Al-rich side. The highest Ni self-diffusion coefficient is not reached for the Ni concentration with the highest liquidus temperature (1940 K for $\text{Al}_{50}\text{Ni}_{50}$), but already at around 40 at. % Ni.

The macroscopic density on Al-Ni melts has been measured as a function of temperature and composition.³¹ The atomic volume calculated by use of the interpolation functions given in Refs. 31–33 for $T=1795$ K are also plotted in the upper part of Fig. 5 (open circles). The average atomic volume shows only a small increase (less than 10%) when increasing the Al concentration for compositions of up to 50 at. % Al. On the Al-rich side, however, the addition of Al leads to a considerably stronger increase in the atomic volume. As suggested by Das *et al.*,¹⁵ for Al-Ni melts the density of packing governs atomic diffusion. We have observed that the Ni self-diffusion coefficient at constant temperature is nearly constant for Ni-rich melts up to Al concentrations of 50 at. % Al. In this composition regime also the atomic volume shows only a very small dependence on the Al con-

centration. At larger Al concentrations the atomic volume strongly increases, which also results in an increase in the Ni self-diffusivity.

Due to the fact that the Ni self-diffusion coefficient is nearly composition independent for Ni-rich Al-Ni melts, during solidification of such melts changes in the Ni concentration in the liquid due to partitioning will not significantly influence the Ni self-diffusivity. This facilitates modeling of the solidification behavior of Ni-rich Al-Ni melts.

IV. CONCLUSIONS

We performed measurements of Ni self-diffusion coefficients in $\text{Al}_{50}\text{Ni}_{50}$ and $\text{Al}_{25}\text{Ni}_{75}$ alloy melts, using quasielastic

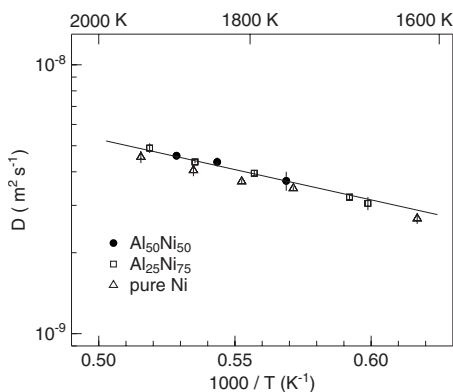


FIG. 4. Ni self-diffusion coefficients in Al-Ni melts. For $\text{Al}_{25}\text{Ni}_{75}$ also the data from previous container experiments (Ref. 17) are included. Also shown are data for pure liquid Ni (Ref. 23). All temperature-dependent diffusivities show an Arrhenius behavior.

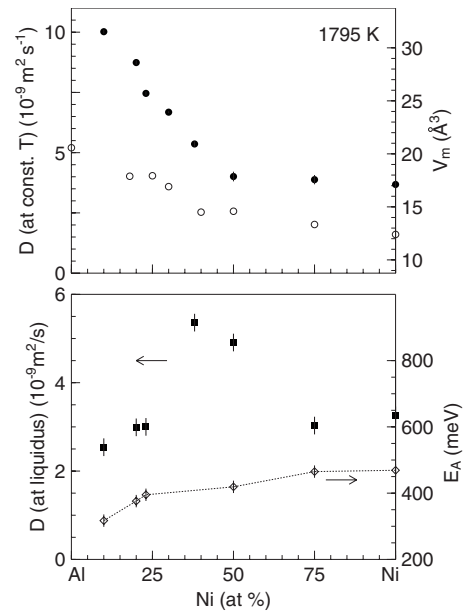


FIG. 5. (Top) Ni self-diffusion coefficients (full circles) as function of composition at 1795 K. Also shown is the atomic volume at 1795 K (open circles) as calculated from the linear interpolation functions given in Refs. 31–33. (Bottom) Ni self-diffusion coefficients at the respective liquidus temperature (squares) and derived activation energy (open diamonds). The dotted line is a guide to the eyes. Diffusion coefficients for Al-rich compounds are from container experiments (Ref. 17).

neutron scattering. This was made possible by the combination of QNS with electromagnetic levitation, which proved to be a veritable tool for dynamical studies, because as a containerless method, it gives access to a large q range, chemically reactive melts, high temperatures and undercooling.

The temperature dependence of the Ni self-diffusivities is well described by an Arrhenius behavior in the investigated temperature range. For the Ni-rich alloys of the Al-Ni system, we found that there is neither a concentration dependence of the Ni self-diffusion coefficient at constant temperature nor a change in the activation energy within experimental errors, up to an Al concentration of 50 at. %. Nevertheless, due to the strong composition dependence of the melting temperature in Al-Ni, the diffusivity values at the liquidus temperature significantly change with composition. For Al-rich alloys investigated in former studies, the Ni self-diffusion coefficients at constant temperatures significantly

increase when adding further Al. The observed composition dependence of the diffusivity corresponds to the composition dependence of the atomic volume. This indicates that the Ni self-diffusivity in liquid Al-Ni is mainly governed by the density of packing. Together with the data of the preceding studies on Al-rich Al-Ni alloys,¹⁷ data on the Ni self-diffusivity as function of the temperature is now available in the full range of composition, providing a basis for a quantitative modeling of the solidification of Al-Ni melts.

ACKNOWLEDGMENTS

We thank F. Yang, A. Meier-Koll, H. Hartmann, and O. Heinen for their help during the measurements and J. Horbach for fruitful discussions. We acknowledge financial support by the German DFG (SPP Phasenumwandlungen in mehrkomponentigen Schmelzen) under Grants No. Me 1958/2-3 and No. Ho1942/6-3.

-
- ¹M. Rappaz and W. J. Boettinger, *Acta Mater.* **47**, 3205 (1999).
²W. J. Boettinger, J. A. Warren, C. Beckermann, and A. Karma, *Annu. Rev. Mater. Res.* **32**, 163 (2002).
³R. Heringer, C. A. Gandin, G. Lesoult, and H. Henein, *Acta Mater.* **54**, 4427 (2006).
⁴M. Asta, C. Beckermann, A. Karma, W. Kurz, R. Napolitano, M. Plapp, G. Purdy, M. Rappaz, and R. Trivedi, *Acta Mater.* **57**, 941 (2009).
⁵K. Eckler, R. F. Cochrane, D. M. Herlach, B. Feuerbacher, and M. Jurisch, *Phys. Rev. B* **45**, 5019 (1992).
⁶H. Hartmann, P. K. Galenko, D. Holland-Moritz, M. Kolbe, D. M. Herlach, and O. Shuleshova, *J. Appl. Phys.* **103**, 073509 (2008).
⁷M. Barth, B. Wei, and D. M. Herlach, *Phys. Rev. B* **51**, 3422 (1995).
⁸S. Reutzel, H. Hartmann, P. K. Galenko, S. Schneider, and D. M. Herlach, *Appl. Phys. Lett.* **91**, 041913 (2007).
⁹A. Kerrache, J. Horbach, and K. Binder, *EPL* **81**, 58001 (2008).
¹⁰D. M. Herlach, P. Galenko, and D. Holland-Moritz, in *Metastable Solids from Undercooled Melts*, Pergamon Materials Series, edited by R. W. Cahn (Elsevier, Oxford, 2007).
¹¹H. J. V. Tyrrell and K. R. Harris, *Diffusion in Liquids* (Butterworths, London, 1984).
¹²A. Meyer, *Phys. Rev. B* **66**, 134205 (2002).
¹³A. Griesche, M. P. Macht, S. Suzuki, K.-H. Kraatz, and G. Froberg, *Scr. Mater.* **57**, 477 (2007).
¹⁴M. Maret, T. Pomme, A. Pasturel, and P. Chieux, *Phys. Rev. B* **42**, 1598 (1990).
¹⁵S. K. Das, J. Horbach, M. M. Koza, S. Mavila Chathoth, and A. Meyer, *Appl. Phys. Lett.* **86**, 011918 (2005).
¹⁶M. S. Petrushevskii, E. C. Levin, and P. V. Geld, *Russ. J. Phys. Chem.* **45**, 1719 (1971).
¹⁷S. Mavila Chathoth, A. Meyer, M. M. Koza, and F. Juranyi, *Appl. Phys. Lett.* **85**, 4881 (2004).
¹⁸L. Do Phuong, D. Nguyen Manh, and A. Pasturel, *Phys. Rev. Lett.* **71**, 372 (1993).
¹⁹M. Asta, D. Morgan, J. J. Hoyt, B. Sadigh, J. D. Althoff, D. de Fontaine, and S. M. Foiles, *Phys. Rev. B* **59**, 014271 (1999).
²⁰J. Horbach, S. K. Das, A. Griesche, M.-P. Macht, G. Froberg, and A. Meyer, *Phys. Rev. B* **75**, 174304 (2007).
²¹D. M. Herlach, *Annu. Rev. Mater. Sci.* **21**, 23 (1991).
²²D. Holland-Moritz, T. Schenk, P. Convert, T. Hansen, and D. M. Herlach, *Meas. Sci. Technol.* **16**, 372 (2005).
²³A. Meyer, S. Stüber, D. Holland-Moritz, O. Heinen, and T. Unruh, *Phys. Rev. B* **77**, 092201 (2008).
²⁴T. Unruh, J. Neuhaus, and W. Petry, *Nucl. Instrum. Methods Phys. Res. A* **580**, 1414 (2007).
²⁵A. Meyer, J. Horbach, O. Heinen, D. Holland-Moritz, and T. Unruh, *Defect Diffus. Forum* **289-292**, 609 (2009).
²⁶D. Holland-Moritz, S. Stüber, H. Hartmann, T. Unruh, T. Hansen, and A. Meyer, *Phys. Rev. B* **79**, 064204 (2009).
²⁷J. P. Hansen and I. R. McDonald, *Theory of Simple Liquids* (Academic, London, 1976).
²⁸J. P. Boon and S. Yip, *Molecular Hydrodynamics* (McGraw-Hill, New York, 1980).
²⁹U. Balucani and M. Zoppi, *Dynamics of the Liquid State* (Clarendon, Oxford, 1994).
³⁰K. Binder and W. Kob, *Glassy Materials and Disordered Solids: An Introduction to their Statistical Mechanics* (World Scientific, Singapore, 2005).
³¹Y. Plevachuk, I. Egry, J. Brillo, D. Holland-Moritz, and I. Kaban, *Int. J. Mater. Res.* **98**, 107 (2007).
³²J. Brillo and I. Egry, *Z. Metallkd.* **95**, 691 (2004).
³³J. Brillo, I. Egry, and J. Westphal, *Int. J. Mater. Res.* **99**, 162 (2008).